SEISMIC PERFORMANCE OF HIGH-STRENGTH REINFORCED CONCRETE COLUMNS AFTER FIRE EXPOSURE

Bo-Jun HUANG[1], and Chung-Chan HUNG[2], Rong-Jing WANG[3], Shun-Chih WANG[4], Ming-Yuan LEI[5], and Chi-Chung LEE[6]

SUMMARY

In this study, a total of 4 high-strength reinforced concrete column specimens were made, 2 of which were subjected to a 2-hour fire exposure test according to standard heating conditions, and the other 2 were used as a control group without exposure to fire. All specimens were subjected to cyclic loading tests to discuss fire effect on seismic performance. The test results show that for the specimens with the design compressive strength of 35 and 70 MPa, the maximum lateral strength after fire damage were decreased by 7.8 and 13%, respectively, and the effective stiffness were decreased by 48 and 55%, respectively. It is found that 2-hour fire exposure has little effect on the maximum lateral strength for high-strength reinforced concrete, and the reduction in effective stiffness is similar for the specimens using general and high-strength concrete.

Keywords: *SEEBUS; high-strength rebar; high-strength concrete; columns; fire exposure; seismic performance.*

INTRODUCTION

With the development of structural material technology and the increase in the demand for high-rise buildings, related research on high-strength reinforced concrete has been continuously developed at home and abroad in recent years. There is still a lack of research on the impact on the seismic performance of high-strength reinforced concrete after fire damage while fires and earthquakes have always been the main causes of building damages. Therefore, this study aims to evaluate the residual seismic capacity of high-strength reinforced concrete column members after fire damage, which is discussed by the test results of 2-hour fire exposure test and cyclic loading test.

The literature (Wang 2017) points out that high-strength concrete material has physical properties such as denser microstructure and lower permeability compared to general-strength concrete, which leads to the inability of the concrete to immediately release the water vapor pressure generated by the high-temperature gasification of water molecules, and the internal pressure will continue to rise until the concrete cannot withstand this pressure, causing explosive spalling of the concrete without warning, while general-strength concrete has failure pattern of slowly spalling on the concrete surface (Chung 2020). Therefore, it is necessary to study the residual seismic capacity of high-strength reinforced concrete after fire damage due to the different effect on general-strength and high-strength reinforced concrete caused by fire.

Some literatures (Liu 2021) point out that the seismic capacity of reinforced concrete structures after fire damage can be evaluated through the isotherms distribution of the section. For example, Eurocode provides the 500°C

[1] *Graduate Student, Department of Civil Engineering, National Cheng Kung University, Taiwan, e-mail: n66104131@gs.ncku.edu.tw*
[2] *Professor, Department of Civil Engineering, National Cheng Kung University, Taiwan, e-mail: cchung@mail.ncku.edu.tw*
[3] *Director General, Architecture and Building Research Institute, Ministry of the Interior, Taiwan*
[4] *Director, Diaster Prevention Division, Architecture and Building Research Institute, Ministry of the Interior, Taiwan*
[5] *Research Fellow, Architecture and Building Research Institute, Ministry of the Interior, Taiwan*
[6] *Associate Research Fellow, Architecture and Building Research Institute, Ministry of the Interior, Taiwan*

isotherm method, which makes the assumptions that concrete outside the 500°C isotherm is considered to be ineffective, while the concrete within the 500°C isotherm is considered complete and provides the original strength. It can be seen that the isotherm distribution of the section is an important indicator of the fire damaged structure and this study will also provide the isotherm distribution for reference.

DESIGN OF COLUMN SPECIMENS

A total of 4 single-column specimens were made in this study, which is shown in Figure 1. The specimens were divided into 2 groups in terms of design compressive strength of concrete, which is general-strength 35 MPa and high-strength 70 MPa, respectively. In each group, 1 specimen was subjected to 2-hour fire exposure test, and the other was the control group which was not subjected to fire test. In addition, except for the design compressive strength of concrete, the other configurations of the 4 specimens were the same, and columns were designed for single curvature with 15% axial compression ratio, which is shown in Table 1.

Figure 1 Photo of the specimens

Table 1 Design variables of specimens

Specimen	N35	F35	N70	F70
Design compressive strength of concrete [MPa]	35	35	70	70
Applied axial load [kN]	840	840	1680	1680
Fire exposure duration [hr]	0	2	0	2

The section of 4 specimens were designed to the same, which has the size of 40×40 cm with 4 cm cover thickness and 120 cm column hight, design yield strength of 550 MPa with 8-#8 rebars for longitudinal bars and design yield strength of 790 MPa with 3-#4 rebars and with a spacing of 6.5 cm, as shown in Figure 2(a).

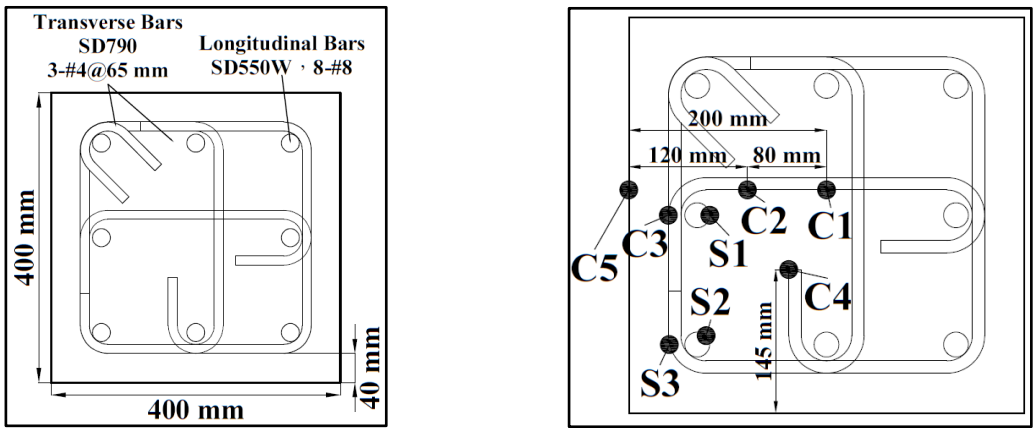

(a) Section design (b) Thermocouple design

Figure 2 Section configuration of specimens

For the purpose of measuring the temperature distribution of the section, the fired specimen F35 and F70 were preinstalled the thermalcouples before concrete grouting, which is used to evaluate the damaged condition of the

section after fire exposure. The position and number of the thermocouples are shown in Figure 2(b), which were installed on the section from the column base to the top of the 1st, 3rd, 5th, and 7th layers of stirrups, and each section is equipped with 8 thermocouples, including 5 concrete temperature measuring points C1 to C5, which are column center, a quarter column depth, cover depth, half depth between column center and corner reinforcement and concrete surface, respectively; 3 steel reinforcement temperature measuring points S1 to S3, which are general rebar, corner rebars and stirrups, respectively. In addition, the thermocouples in this study uses K-type temperature measuring line, which can measure the temperature range from -200 to 1200 °C, and the temperature error range from 1.5 to 2.5 °C, which is the most widely used type of thermocouple at present.

Material Test

In this study, 28-day and cyclic loading test day of concrete compressive strength were tested and is shown in Table 2. For the concrete of design compressive strength of 35 and 70 MPa, average compressive strengths are 39.0 and 66.9 MPa for 28-day, respectively, and 46.7 and 86.6 MPa for cyclic loading test day, which has concrete age of 105 and 112 days, respectively. In addition, the fired specimens F35 and F70 were subjected to the fire test before cyclic loading test, therefore, there was no compressive test data for the cyclic loading test day of fired specimens.

For the steel materials, 2 groups of steel tensile tests were carried out, which is SD550W for longitudinal bars and SD790 for transverse bars and is shown in
Table 3. Each average yield strengths is 576 and 844 MPa, respectively, and each average tensile strengths is 749 and 1018 MPa, which has yield to tensile ratio of 1.3 and 1.21, respectively , and each elongation is 12 and 11%, respectively.

Table 2 Average compressive test of concrete

Specimen	N35	F35	N70	F70
28 days compressive strength [MPa]	39.0	39.0	66.9	66.9
Compressive strength of cyclic loading test day [MPa]	46.7	N/A	86.6	N/A

Table 3 Average tensile test of rebars

Rebar	Part	Yield strength [MPa]	Tensile strength [MPa]	Elogation [%]
SD550W	Longitudinal bars	576	749	12
SD790	Transverse bars	844	1018	11

EXPERIMENTAL PROGRAM

2-Hour Fire Exposure Test

This study plans to carry out the fire tests of F35 and F70 specimens in a refractory furnace. The specimens will be uniformly heated by liquid petroleum gas in the furnace without applying axial force. The heating method is in accordance with the heating curve of CNS12514-1 by 2 hours, which is the national standard in Taiwan, and the temperature is followed by equation (1). After the fire test was terminated, the specimen was removed from the refractory furnace after the temperature was lowered to room temperature by natural cooling.

$$T = 345(8t + 1) + 20 \quad (1)$$

Where, T is the temperature in terms of °C and t is the fire duration in terms of min.

In order to prevent the damage of the upper and lower bases of the single-column specimens during the fire test, 2 layers of ceramic fiber fireproof cotton with a total thickness of 7.5 cm will be pasted on the surface of the upper and lower bases before the experiment. In addition, to reduce the insulation effect caused by fireproof cotton on the plastic hinge area of the specimens, fireproof cotton will not be pasted on the area near the column by half column width (20 cm), as shown in Figure 3.

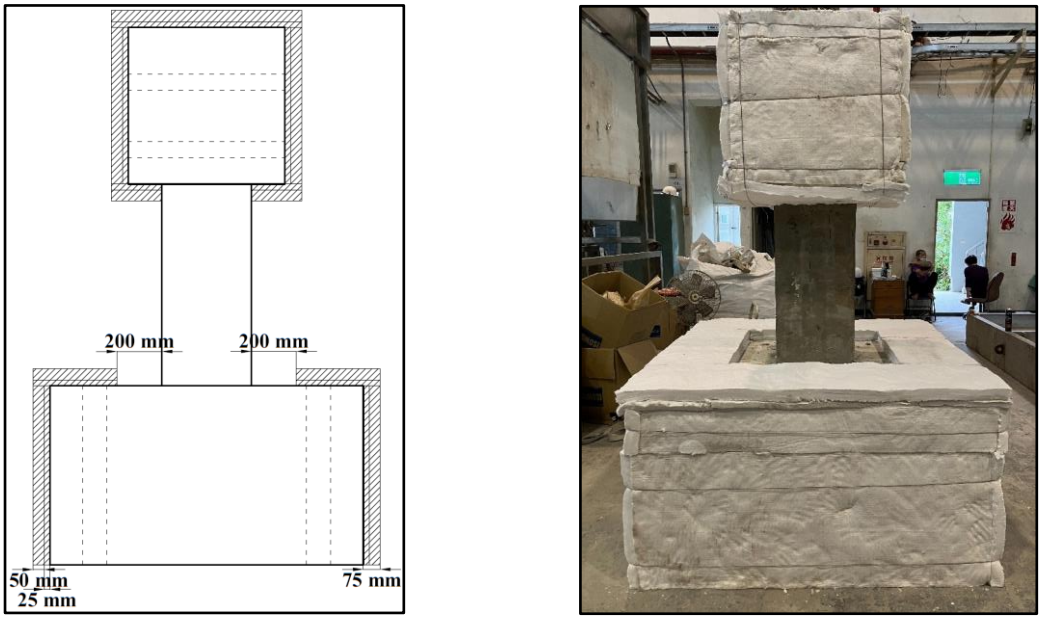

(a) Design (b) Photo in situ

Figure 3 Configuration of ceramic fiber fireproof cotton

Cyclic Loading Test

In this study, cyclic loading tests were carried out in conjunction with reaction wall and strong floor, and the seismic behavior of the specimens were evaluated by the hysteresis loops and failure patterns from the tests. The experimental setup is shown in Figure 4, which includes a 1000-kN horizontal actuator in the lateral side and a set of 2000-kN axial force jack on the top. The test will first load vertically to the target axial force and then control the top of the column to reach the specified drift ratio by displacement control method. The target drift ratio are 0.25, 0.375, 0.5, 0.75, 1, 1.5, 2, 3, 4, 5, 6, 7 and 8%, respectively, and each drift ratio is carried out for two cycles, as shown in Figure 5. In addition to the displacement sensor of the horizontal actuator, an additional optical measurement system was set up to obtain more accurate displacement datas in this study. The optical measurement system uses the NDI Optotrak Certus instrument of Northern Digital Incorporation (hereinafter referred to as NDI), which principle is to send a signal by the NDI host to the sensors pasted on the surface of the specimens, and receive its reflected signal to record the coordinates.

Figure 4 Setup of cyclic loading tests

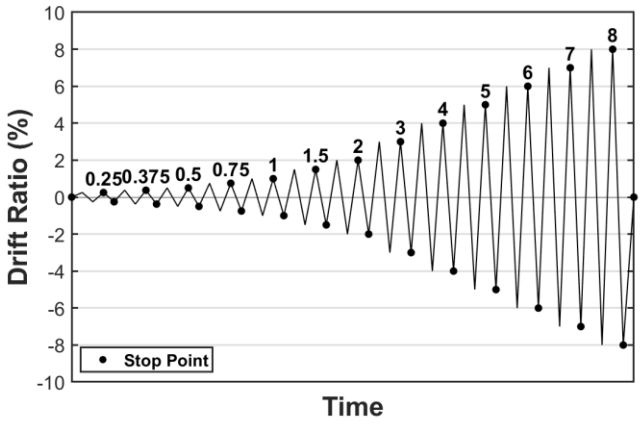

Figure 5 Drift history of cyclic loading tests

RESULTS AND DISCUSSION

2-Hour Fire Exposure Test

Both F70 and F35 specimens were successfully completed the 2-hour fire exposure test, which has 4.5 and 4.0% of moisture content in concrete surface before the experiment and 69 and 76 days of concrete age, respectively. The comparison between the furnace temperature history and the standard heating curve is shown in Figure 6, which can be seen that the experimental heating conditions are consistent with the standard heating curve of the experimental program.

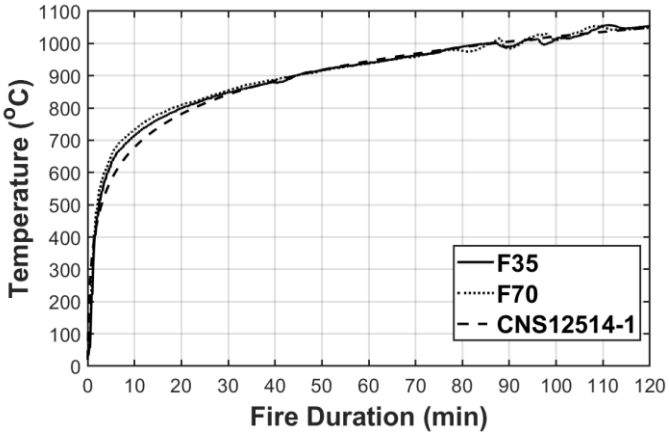

Figure 6 Heating curve of Furnace

The severely damaged surfaces of F35 and F70 specimens after fire test are shown in Figure 7. From the interface between the lower base and the shaft, it can be seen that the color of the concrete surface after exposure to fire will change from gray to yellowish brown, and it can also be seen that there are many cracks on the concrete surface, which do not penetrate the shaft and they are arranged in sheets for the surface of F70 specimens, and the moisture content in the concrete surface of both specimens after the experiment are almost 0, therefore, it is judged that these cracks are caused by shrinkage of the concrete due to the loss of moisture. In addition, F70 specimen can clearly observe the moment of explosive spalling on concrete surface during the experiment, and it can be seen from Figure 7(c)(d) that the concrete spalling is serious and stirrups can be seen directly in many places, which means that the spalling depth of concrete has exceeded the thickness of the cover (4 cm). If the duration of the fire keep increasing, the temperature of the rebars which are exposed to fire directly will rise rapidly to cause a large reduction in strength. Compared with the F35 specimen, only a corner of the concrete spalled off, which shows that high-strength concrete is less refractory than general-strength concrete due to the explosive spalling behavior during fire.

(a) East side of F35 (b) North side of N35 (c) East side of F70 (d) North side of F70

Figure 7 The surfaces of the fired specimens after 2-hour fire exposue test

Due to the concrete spalling in the fire test, some thermocouples were damaged by directly exposed to fire, therefore, the complete and smooth temperature datas were selected as the representative heating curve, and the datas had been recorded until 4 hours after the fire test, which is the moment that every measuring point had reached the highest temperature and cooled down slowly, as shown in Figure 8.

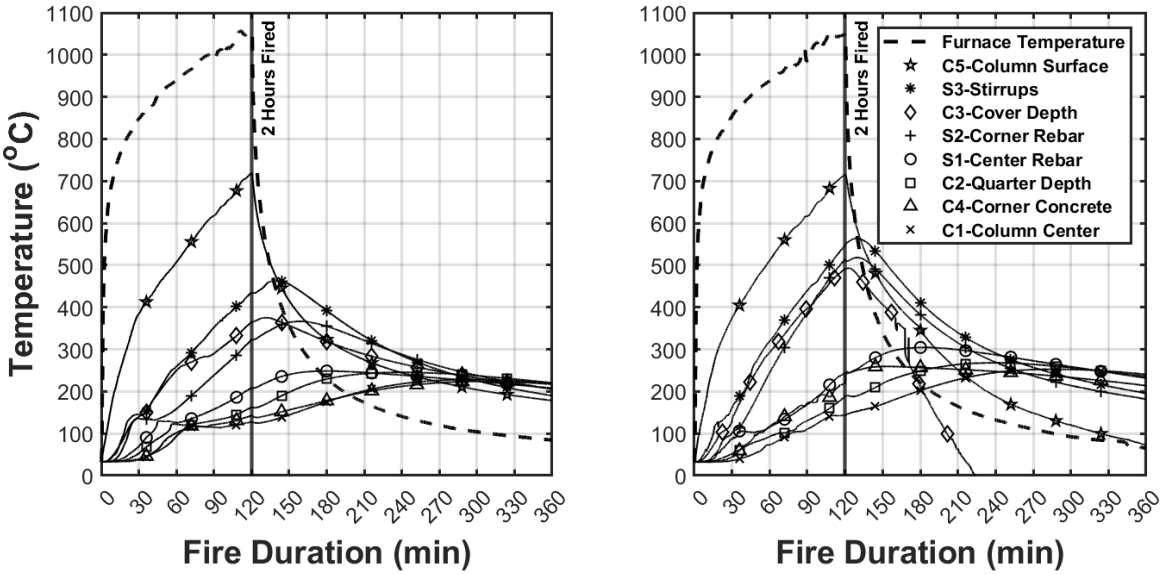

(a) F35 specimen (b) F70 specimen

Figure 8 Representative heating curve of fired specimens

Mark the maximum temperature of each representative heating curve at the position of the corresponding measuring point on the section, as shown in Figure 9. Assume that the temperature of each measuring point can be used as the temperature of its depth, and use linear interpolation to calculate the depth of each 100℃ isotherm. There also assume that the four sides of the specimens were uniformly burned, which causes a symmetric distributed isotherms, therefore, only a quarter section isotherm distribution figure were drawn, as shown in Figure 10. It can be seen that the isotherm distribution of high-strength reinforced concrete section shrinks inwardly compared to the general strength concrete, which means that the overall temperature of the high strength reinforced concrete is higher, and it did have more serious damage duing the fire test.

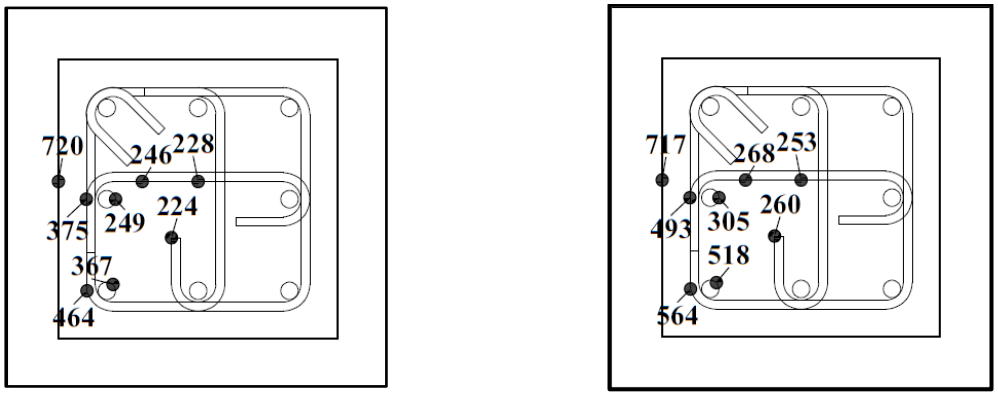

(a) F35 specimen (b) F70 specimen

Figure 9 Maximun temperature on each measuring point of fired specimens [°C]

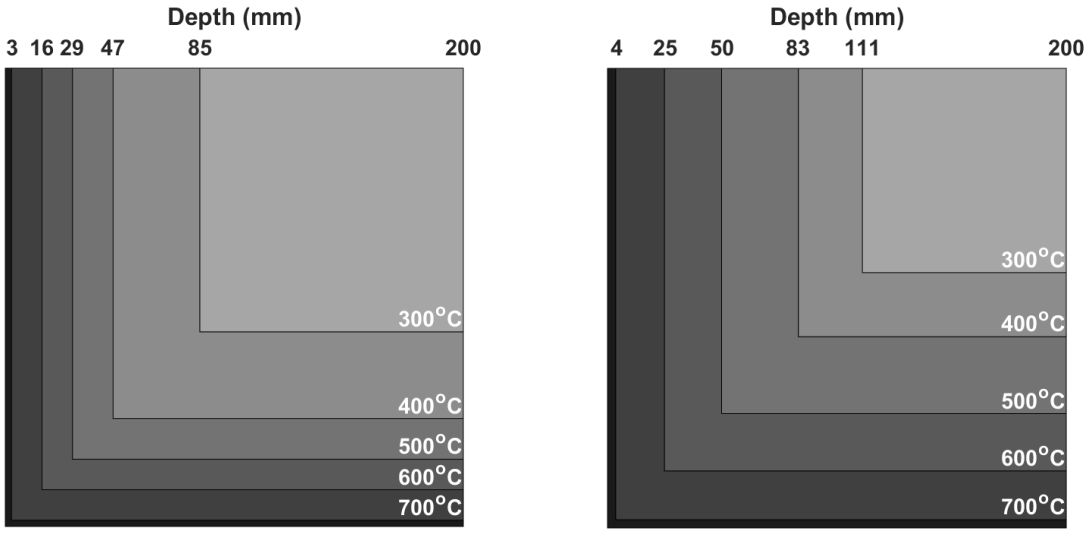

(a) F35 specimen (b) F70 specimen

Figure 10 Each 100°C isotherm of fired specimen on a quarter section

Cyclic Loading Test

The cyclic loading tests of all specimens were carried out to the maximum allowable drift ratio. Among them, high-strength concrete specimens N70 and F70 were only allowed to achieve a drift ratio of 7% due to the limit of the experimental devices, which can not withstand high axial force of 168 tf to reach larger drift ratio, while N35 and F35 specimens have completed the pre-planned maximum drift ratio of 8%. All displacement datas of hysteresis loops were corrected by NDI, as shown in Figure 11, and refer to the Pham et al.'s recommendation (Pham 2022), use the slope of the secant line of 75% of the maximum lateral strength and origin to be the effective stiffness. In addition, this study uses the drift ratio of 85% of the maximum lateral strength at the strength degradation line to be the failure drift ratio.

For N35 specimen, the maximum lateral strengths in positive and negative directions are 396 and 406 kN, respectively, and both occur in the loops of drift ratio of 3%. The effective stiffnesses in positive and negative directions are 29.6 and 24.5 kN/mm, respectively. The positive failure drift ratio is 5.9%, and the lateral strength at the drift ratio of 8% still remains 94% of the maximum lateral strength in negative direction. The failure pattern are shown in Figure 12(a), the cracks developed horizontal flexural cracks before the drift ratio of 0.75%, and developed oblique flexural-shear cracks after the drift ratio of 0.75%, and the concrete was crushed at the drift ratio of 2 and 4% in positive and negative directions, respectively.

For N70 specimen, the maximum lateral strengths in positive and negative directions are 444 and 462 kN, respectively, and both occur in the loops of drift ratio of 1.5%. The effective stiffnesses in positive and negative directions are 38.7 and 32.8 kN/mm, respectively. The negative failure drift ratio is 6.3%, and the lateral strength at the drift ratio of 7% still remains 86% of the maximum lateral strength in positive direction. The failure pattern are shown in Figure 12(b), the cracks developed horizontal flexural cracks before the drift ratio of 0.75%, and

developed oblique flexural-shear cracks after the drift ratio of 0.75%, and the concrete was crushed at the drift ratio of 1.5 and 2% in positive and negative directions, respectively.

For F35 specimen, the maximum lateral strengths in positive and negative directions are 357 and 383 kN, respectively, and occurs in the loops of drift ratio of 4 and 5%, respectively. The effective stiffnesses in positive and negative directions are 14.0 and 14.2 kN/mm, respectively. The lateral strength at the drift ratio of 8% still remain 94 and 99% of the maximum lateral strength in positive and negative direction, respectively. The failure pattern are shown in Figure 12(c), which only added a few cracks during the cyclic loading test and most of them are developed along the existing cracks caused by the fire test, and the concrete was crushed at the drift ratio of 5 and 4% in positive and negative directions, respectively.

For F70 specimen, the maximum lateral strengths in positive and negative directions are 379 and 412 kN, respectively, and occurs in the loops of drift ratio of 3 and 7%, respectively. The effective stiffnesses in positive and negative directions are 16.8 and 15.6 kN/mm, respectively. The lateral strength at the drift ratio of 7% still remain 97 and 100% of the maximum lateral strength in positive and negative direction, respectively. The failure pattern are shown in Figure 12(d), which almost added no crack during the cyclic loading test, and is hard to observe ther developement, and the concrete has no obvious failure moment.

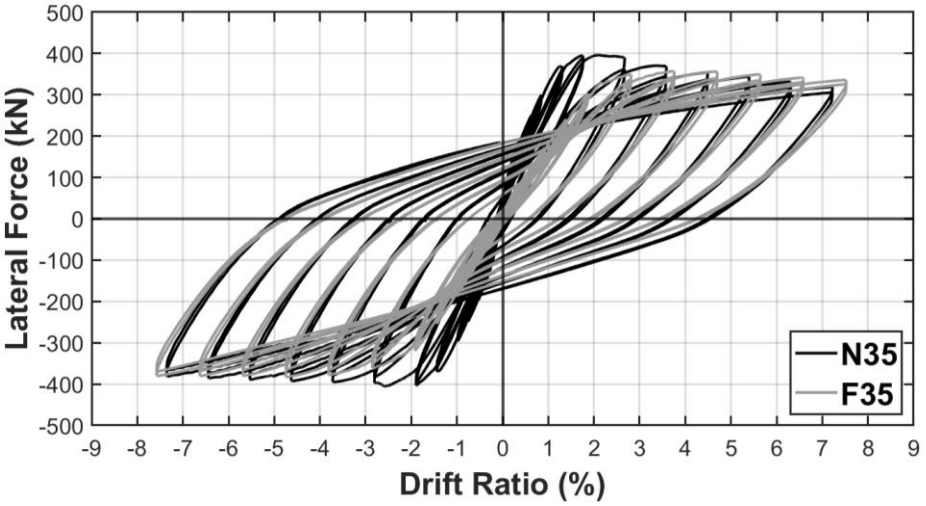

(a) N35 and F35 specimens

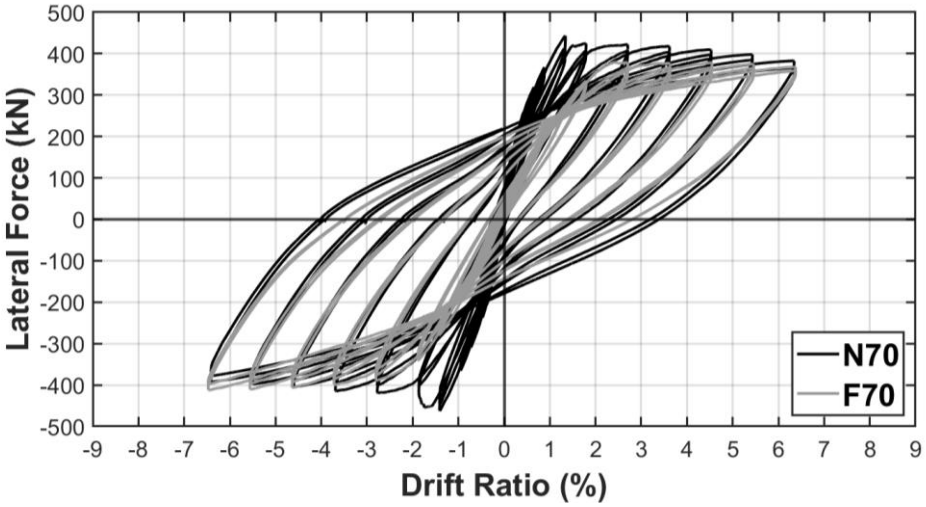

(b) N70 and F70 specimens

Figure 11 Hysteresis loops

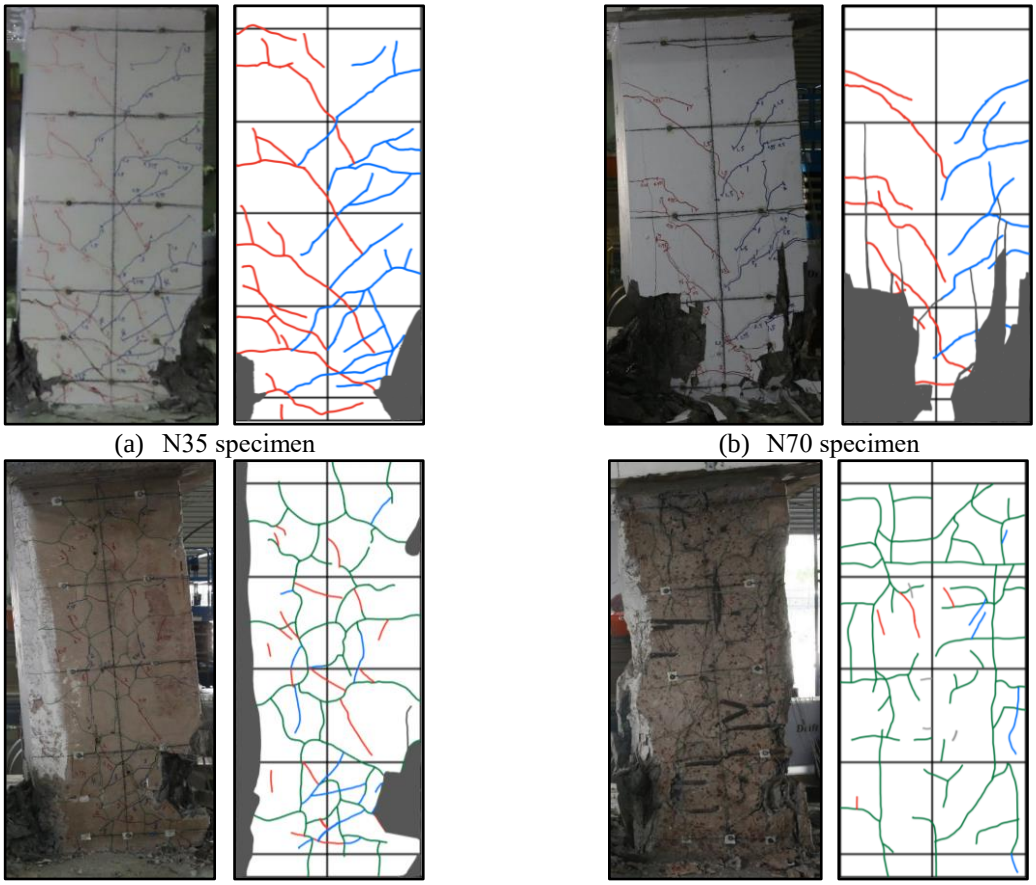

(a) N35 specimen (b) N70 specimen

(c) F35 specimen (d) F70 specimen

Figure 12 Failure patterns

The envelopes of hysteresis loops of all specimens are shown in Figure 13. It can be seen that the envelope of N35 specimen is smoother than N70 specimen, which shows higher hardness and more brittle behavior of high-strength concrete than general-strength concrete. Fired specimens F35 and F70 have no obvious strength degradation line, which is considered to be the reason that cover concrete is already damaged duing fire test and only contribute a little strength, therefore, it causes a little effect on the curve when the cover failure during the later stage of cyclic loading test.

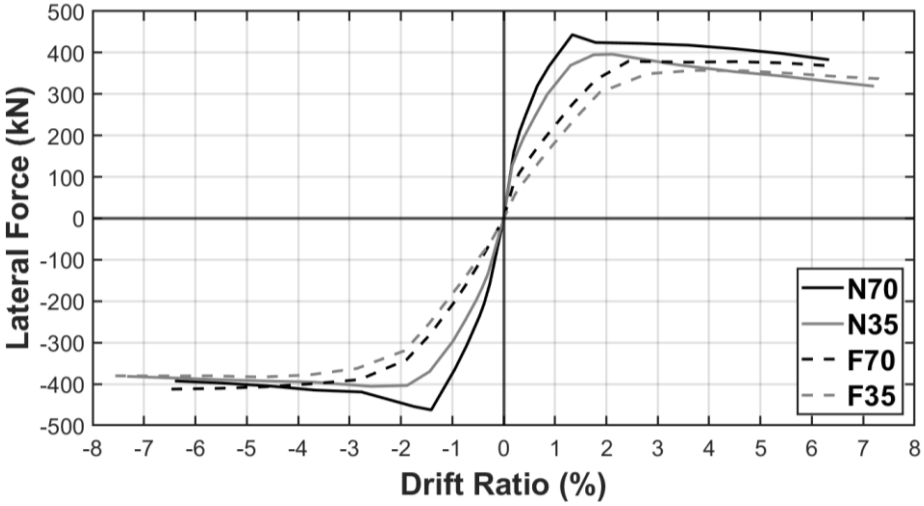

Figure 13 Envelopes of hysteresis loops

The maximum lateral strength and effective stiffness of all specimens use the average of the values in positive and negative directions, and the comparison are shown in Table 4 and Table 5, respectiely. For the concrete design compressive strength of 35 and 70 MPa, the maximum lateral strength decreased by 7.8 and 13%, and the effective

stiffness decreased by 48 and 55%, respectively. It can be found that 2-hour fire exposure has little effect on the maximum lateral strength and the reduction in effective stiffness are similar to the specimens using high-strength and general-strength concrete. In addition, when the design compressive strength of concrete is increased from 35 to 70 MPa and according to the same configuration in this study, the maximum lateral strength and effective stiffness can be increased by 13 and 32%, respectively.

Table 4 Comparison of maximum lateral strength [kN]

	Unfired	Fired	Difference
Compressive strength 35 MPa	401 (N35 specimen)	370 (F35 specimen)	-7.8%
Compressive strength 70 MPa	453 (N70 specimen)	396 (F70 specimen)	-13%
Difference	+13%	+6.9%	N/A

Table 5 Comparison of effective stiffness [kN/mm]

	Unfired	Fired	Difference
Compressive strength 35 MPa	27.0 (N35 specimen)	14.1 (F35 specimen)	-48%
Compressive strength 70 MPa	35.8 (N70 specimen)	16.2 (F70 specimen)	-55%
Difference	+32%	+15%	N/A

CONCLUSIONS

(1) For the fire response, the use of high-strength concrete will result in a more serious concrete spalling behavior and deeper isotherm distribution due to the denser microstructure property than general-strength concrete.

(2) For the failure patterns, unfired specimens develop flexural cracks to flexural shear cracks, and concrete crushed in the end, while the fired specimens develop the cracks along the cracks caused by the fire test and with no obvious concrete crushing moment. In addition, the use of high-strength concrete will result in concrete crushing at smaller drift ratio than the use of general-strength concrete.

(3) For the envelope of hysteresis loops, fired specimens have no obvious strength degradation line compared to the unfired specimens due to the damaged cover concrete. And the use of high-strength concrete will result in a sharper envelope than the use of general-strength concrete.

(4) For the maximum lateral strength and effective stiffness, for the concrete design compressive strength of 35 and 70 MPa, the maximum lateral strength decreased by 7.8 and 13%, and the effective stiffness decreased by 48 and 55%, respectively.

REFERENCES

Chung, H. Y., Hwang, S. J., Hung, C. C., Liu, K. Y. (2020), "The Study of Seismic-Resistant Performances of Post-Fire RC and Steel Structural Members (1/3)," *Commissioned research projects report, Architecture and Building Research Institute, Ministry of the Interior, ROC (Taiwan)*.

European Committee (2004), *"Eurocode2: Design of concrete structures-Part1-2: General rules-Structural fire design," EN 1992-1-2:2004:E.*

Liu, K. Y., Hwang, S. J., Hung, C. C., Chung, H. Y. (2021), "The Study on the Seismic-Resistant Performances of Post-Fire RC Frame Structure (2/3)," *Commissioned research projects report, Architecture and Building Research Institute, Ministry of the Interior, ROC (Taiwan)*.

Pham P. A. H., Terry YP. Y., Hung, C. C., Khalid M. M. (2022), *"Seismic behaviour of full-scale lightly reinforced concrete columns under high axial loads," Journal of Building Engineering, Volume 56, 104817.*

Wang, T. C. (2017), "The Spalling Behavior of New High Strength Concrete under High Temperature, " *Research project report, Architecture and Building Research Institute, Ministry of the Interior, ROC (Taiwan)*.